MR imaging in children with transverse myelitis and acquired demyelinating syndromes

Ines El Naggar, Robert Cleaveland, Eva-Maria Wendel, Annikki Bertolini, Kathrin Schanda, Michael Karenfort, Charlotte Thiels, Adela Della Marina, Mareike Schimmel, Steffen Leiz, Christian Lechner, Matthias Baumann, Markus Reindl, Andreas Wegener-Panzer, Kevin Rostásy, Nina Barišić, Bettina Behring, Steffen Berweck, Markus Blankenburg, Astrid Blaschek, Christoph Conrad, Katharina Diepold, Matthias Eckenweiler, Astrid Eisenkölbl, Walid Fazeli, Tobias Geis, Annette Hackenberg, Katharina Harms, Andrea Klein, Johannes Koch, Barbara Kornek, Margherita Nosadini, Daniela Pohl, Martin Pritsch, Michela Salandin, Torsten Sandrieser, Stefano Sartori, Johannes Stoffels, Gert Wiegand

MR imaging in children with transverse myelitis and acquired demyelinating syndromes

Ines El Naggar [a], Robert Cleaveland [b], Eva-Maria Wendel [c], Annikki Bertolini [a],
Kathrin Schanda [d], Michael Karenfort [e], Charlotte Thiels [f], Adela Della Marina [g],
Mareike Schimmel [h], Steffen Leiz [i], Christian Lechner [j], Matthias Baumann [j], Markus Reindl [d],
Andreas Wegener-Panzer [b], Kevin Rostásy [a,*], on-behalf-of-the-BIOMARKER-Study-Group [#]

[a] *Department of Pediatric Neurology, Children's Hospital Datteln, University Witten/Herdecke, Datteln, Germany*
[b] *Department of Pediatric Radiology, Children's Hospital Datteln, University Witten/Herdecke, Datteln, Germany*
[c] *Division of Pediatric Neurology, Department of Pediatrics, Olgahospital, Stuttgart, Germany*
[d] *Medical University Innsbruck, Innsbruck, Austria*
[e] *Clinic of General Pediatrics, Neonatology and Pediatric Cardiology, Düsseldorf University Hospital, Heinrich-Heine-University, Düsseldorf, Germany*
[f] *Division of Pediatric Neurology, Clinic of Pediatrics, St. Josef-Hospital, Ruhr-University Bochum, Bochum, Germany*
[g] *Department of Pediatric Neurology, Centre for Neuromuscular Disorders, Centre for Translational Neuro- und Behavioral Sciences, University Duisburg-Essen, Essen, Germany*
[h] *Division of Pediatric Neurology, Clinic of Pediatrics, Augsburg University Hospital, University of Augsburg, Augsburg, Germany*
[i] *Division of Pediatric Neurology, Clinic of Pediatrics, Klinikum Dritter Orden, München, Germany*
[j] *Division of Pediatric Neurology, Department of Pediatrics I, Medical University of Innsbruck, Innsbruck, Austria*

* Corresponding author at: Pediatric Neurology, Witten/Herdecke University, Children's Hospital Datteln, Dr. Friedrich-Steiner Str. 5, D-45711 Datteln, Germany
E-mail address: k.rostasy@kinderklinik-datteln.de (K. Rostásy).
[#] Included in the BIOMARKER Study Group.

1. Introduction

Transverse myelitis (TM) is an inflammation of the spinal cord defined by the presence of clinical signs suggestive of spinal cord involvement, typical magnetic resonance imaging (MRI) findings and laboratory features such as increased cerebrospinal fluid (CSF) cell count or the presence of CSF oligoclonal bands (OCBs). Patients with TM develop a (sub-)acute loss of sensory, motor and/or autonomous functions attributed to the affected segment (Proposed diagnostic 2002, Wolf et al., 2012, Barakat et al., 2015).

TM can occur as an isolated inflammation of the spinal cord or be part of autoimmune-mediated diseases such as neuromyelitis optica spectrum disorders (NMOSD) with or without aquaporin-4 antibodies (AQP4-IgG), paediatric multiple sclerosis (pedMS) or myelin oligodendrocyte glycoprotein antibody associated disorders (MOGAD) (Absoud et al., 2016, Hennes et al., 2017). In particular children with serum MOG antibodies (MOG-IgG) can present with isolated TM or as part of a more complex presentation of MOGAD (Hennes et al., 2017, Hacohen et al., 2015). Recognising TM within the spectrum of MOGAD is important as therapy options and prognosis differ from other causes of TM (Hennes et al., 2017, Spadaro et al., 2016).

MRI of patients with TM usually reveal signal alterations in the spinal cord which can be restricted to one up to more than three vertebral segments, the latter being termed longitudinally extensive transverse myelitis (LETM). Previous studies with children have already shown that LETM can be found more likely in patients with MOGAD or NMOSD and less likely in MS patients (Baumann et al., 2018, Dubey et al., 2019, Hacohen et al., 2017). Depending on the underlying disease, lesions are located more often either in the cervical, thoracic, lumbar region or in the conus (Dubey et al., 2019, Fadda et al., 2021). Dubey et al. showed that spinal MRIs of MOG-IgG positive children have a conus involvement in 41% (Dubey et al., 2019). Fadda et al. also recently described a more frequent involvement of the conus in MOGAD compared to MS (Fadda et al., 2021). However, according to Lechner et al. conus lesions were no special feature for MOG-IgG children compared to seronegative children (Lechner et al., 2016).

Fadda et al. also found that leptomeningeal enhancement is a feature of MOG-IgG positive patients in addition to spinal nerve root enhancement (Fadda et al., 2021). These features have not been described by other studies. Regarding ADS and MRI presentation of brain lesions, several studies could show that MRI is a helpful tool in distinguishing between different disease entities as long as antibody or other laboratory results are still pending (Baumann et al., 2018, Hacohen et al., 2017). Larger multi-center studies focusing on the spinal MRI features of children with a TM as part of an ADS are rare, especially regarding MOG-IgG positive children in comparison to other disease entities.

Therefore, the primary objective of our study was to delineate the spectrum of children with a first acquired demyelinating syndrome (ADS) associated with TM, with a special focus on MRI features, especially of children harbouring serum MOG-IgG. Furthermore, we wanted to see if previously described MRI features of these different disease entities are reproducible in our large multi-center cohort.

2. Patients and methods

2.1. Patients

Between 2009 and 2021 1235 children with a suspected ADS were sent to our attention from 60 different mainly European medical centers for testing of serum MOG-IgG and AQP4-IgG and included in an ongoing prospective study (i.e. the BIOMARKER cohort).

For the purpose of this study children referred with a presumed diagnosis of TM either alone (isolated TM) or as part of a broader, more complex clinical presentation were selected and then included if the following data were available: (1) clinical details of the initial event, (2) MRI study of the spine at disease onset and before steroid treatment, (3) serum MOG-/AQP4-IgG status, and (4) cerebrospinal fluid (CSF) testing for cell count and/or OCBs. Patients with infectious aetiologies were excluded from this study.

After review of the data base 111 children were identified as possible candidates. After analysing the initial clinical data and MRI studies, 11 children were excluded for the following reasons: (1) five children had no MRI examination of the whole spine; (2) in two patients the spinal MRI study was not performed at onset; (3) four children were subsequently diagnosed with other conditions including Guillain-Barré syndrome (GBS), neuroborreliosis or anti-N-methyl-D-aspartate (NMDA)-receptor encephalitis. Finally, 100 patients were included in our study. The process of inclusion and exclusion is depicted in Fig. 1. These 100 patients were from 37 different referring medical centers and 7 different countries (Germany (n=76), Austria (n=10), Italy (n=6), Switzerland (n=3), Canada (n=3), Sweden (n=1), and Croatia (n=1)).

2.2. MR imaging

MRI scans were scored independently by two neuroradiologists (AWP, RC) who were blinded to the clinical and serological status of the patient. In case of discordant results, the MRIs were reviewed jointly, and a consensus decision was made. MRIs have been performed on 19 different MRI scanners (spinal MRIs on Philips Intera 1.5 Tesla, Philips Achieva 1.5 Tesla, Philips Achieva 3 Tesla, Philips Ingenia 1.5 Tesla, Philips Ingenia 3 Tesla, Siemens Avanto 1.5 Tesla, Siemens Symphony 1.5 Tesla, Siemens Skyra 3 Tesla, Siemens Aera 1.5 Tesla, Siemens Prisma 3 Tesla, Siemens Sonata 1.5 Tesla, Siemens Trio 3.0, GE Signa 1.5 Tesla, GE Optima 1.5 Tesla, GE Disc 1.5 Tesla and brain MRIs on Philips Intera 1.5 Tesla, Philips Achieva 1.5 Tesla, Philips Achieva 3 Tesla, Philips Panorama 1 Tesla, Philips Ingenia 1.5 Tesla, Philips Ingenia 3 Tesla, Siemens Avanto 1.5 Tesla, Siemens Symphony 1.5 Tesla, Siemens Skyra 3 Tesla, Siemens Aera 1.5 Tesla, Siemens Prisma 3 Tesla, Siemens Harmony 1 Tesla, Siemens Sonata 1.5 Tesla, GE Signa 1.5 Tesla, GE Signa 3 Tesla, GE Disc 1.5 Tesla, GE Disc 3 Tesla).

In all patients a spinal cord MRI was performed during the initial investigations including the following sequences in the majority of
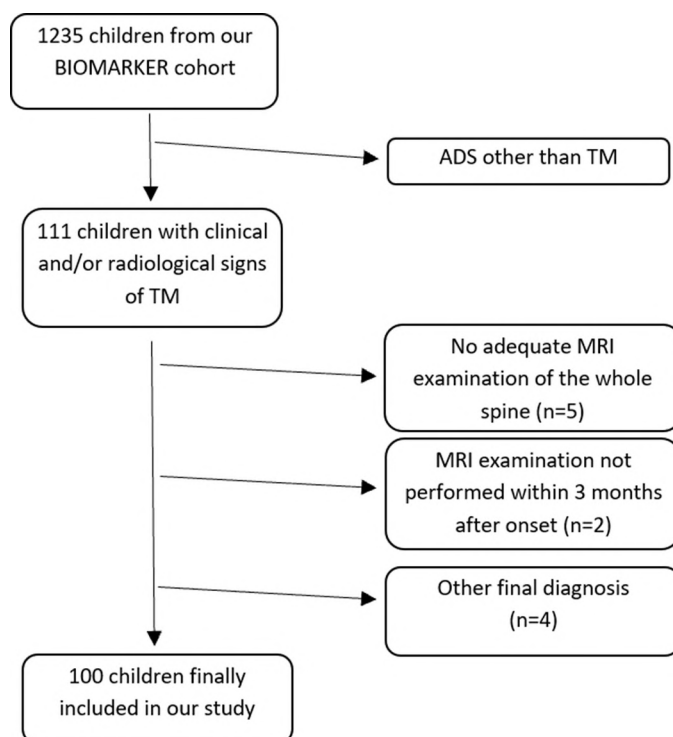

Fig. 1. Process of inclusion and exclusion

patients: sagittal T2 (n=100), axial T2 (n=97), contrast enhanced sagittal T1 (n=84). Those patients, who did not have axial T2 or contrast enhanced sagittal T1 images, were excluded from that respective evaluation. In 86/100 children the initial MRI was performed on scanners with field strength of 1.5 Tesla and in 14/100 children with 3.0 Tesla scanners.

Brain MRI studies from disease onset were available from 94 children with following sequences in the majority of children: axial T2 (n=94), axial FLAIR (n=94), sagittal T2 (n=94), diffusion restriction (n=89) and contrast enhanced axial T1 (n=81). From the other 6/100 patients only the report of the cerebral MRI studies was available and were therefore not included in the evaluation of the brain MRIs.

Spinal MRIs were analysed regarding location of the respective lesions referring to the level of the affected segments (cervical, thoracic, conus medullaris, and mixed) as well as axial cord involvement (white matter only, grey matter only, and mixed) with TSE (turbo spin echo) and SE (spin echo) sequences. Furthermore, the longitudinal extension of spinal lesions was either classified as (1) single short segment (i.e. shorter than three segments), (2) multiple short segments, (3) LETM, (4) whole cord confluent or (5) different extensions in the same study. Lastly, spinal MRIs were assessed for the presence of Gadolinium (Gd) enhancement including leptomeningeal and nerve root enhancement, cavitation, edema, and signal alterations in T1. These features were scored as (1) not present, (2) present and (3) not applicable (e.g. when no Gd was given).

Cerebral MRIs were screened for the total number of brain lesions and allocated into three groups including (1) no or only small non-specific lesions, (2) 1-10 lesions or (3) more than 10 lesions. In addition, the number of supra- and infratentorial lesions was counted as well as the involvement of corpus callosum, deep grey matter (thalamus and/or basal ganglia), brainstem, cerebellum, and periventricular white matter. Furthermore, lesions were assigned to one of the following qualities: (1) predominantly poorly demarcated lesions involving grey and/or white matter, (2) extensive confluent white matter changes, (3) predominantly well-demarcated white matter lesions (MS-like), and (4) mixed qualities. The size of the lesions was assessed with the measurement tool of the PACS software and categorised as (1) smaller than 2 cm, (2) 2 cm or larger or (3) both sizes mixed (smaller and larger than 2 cm). In addition, the following features were analysed: occurrence of T1-hypointense lesions, lesions with Gd enhancement, and lesions of restricted diffusion (high signal on DWI and low signal on ADC).

2.3. Antibody assay

All serum samples were obtained at disease onset and analysed for the presence of MOG-IgG and AQP4-IgG by live cell-based immunofluorescence assays using the protocols as previously described (Mader et al., 2011). MOG-IgG were tested using the alpha-1 isoform of full-length MOG and IgG (heavy and light chain, Dianova) specific secondary antibodies. Screening was performed at dilutions of 1:20 and 1:40 by at least two independent clinically blinded investigators (KS, MR). To determine the end-point titers, positive serum samples were further diluted in two-fold increments. Titer levels of ≥1:160 were classified as MOG-IgG positive as previously described (Mader et al., 2011). Using heavy chain specific secondary antibodies for IgM and IgG (Dianova) we excluded an isolated IgM reactivity in borderline (1:160 and 1:320) seropositive samples. Patients with MOG-IgG were always negative for AQP4-IgG and vice versa.

2.4. Statistical Analysis

Groups were compared using Mann Whitney U, Kruskal Wallis, Chi square or Fisher's exact tests. Statistical significance was defined as two-sided p-value <0.05. P-values were corrected for multiple comparisons using Bonferroni's correction for multiple comparisons. Statistical analyses were performed using IBM SPSS software (IBM SPSS Statistics;

Version 26.0. Armonk, NY: IBM Corp.) or GraphPad Prism 9 (GraphPad Software, La Jolla, CA).

2.5. Standard Protocol Approvals, Registrations and Patient Consents

This study was approved by the Ethics committee of Witten/Herdecke University, Germany as well as the Ethics committee of Medical University Innsbruck, Austria, and all caregivers gave informed consent.

3. Results

Children presenting with TM and a complete data set were included (Fig. 1). The cohort of 100 children consisted of 54 female and 46 male patients with a median age at onset of 10.5 years (age range eight months – 17 years). All children had radiological signs, laboratory features and clinical symptoms of TM, such as sensory loss, motor function loss and/or bladder/bowel dysfunction. CSF cell count was available in 93/100 patients and 93/100 children were tested for OCBs. Every child in our cohort who has not been tested for OCBs has been tested for cell count and vice versa.

3.1. Clinical characterisation of children with MOGAD, NMOSD, MS and double seronegative TM

For further analysis we assigned the patients to four groups depending on the antibody status, diagnosis of MS or NMOSD (Fig. 2). 33 children had positive serum MOG-IgG with a median titer of 1:2150 (range 1:160-1:10560), (group 1: MOGAD, including TM, LETM, acute disseminated encephalomyelitis (ADEM) and NMOSD-MOGAD). Seven children had NMOSD according to the international consensus diagnostic criteria for NMOSD 2015 (Wingerchuk et al., 2015) including six children with AQP4-IgG (group 2: NMOSD). 34 children had a TM/LETM and were MOG-IgG and AQP4-IgG negative including three children with ADEM (group 3: double seronegative TM). 26 children had MS: 25 were diagnosed with MS at the initial event according to the revised McDonald criteria 2017 (Thompson et al., 2018) and one child was diagnosed with a clinically isolated syndrome (CIS) and TM but developed a second clinical episode (group 4: MS). No patient with MS had serum MOG-IgG. The demographical features are shown in Table 1.

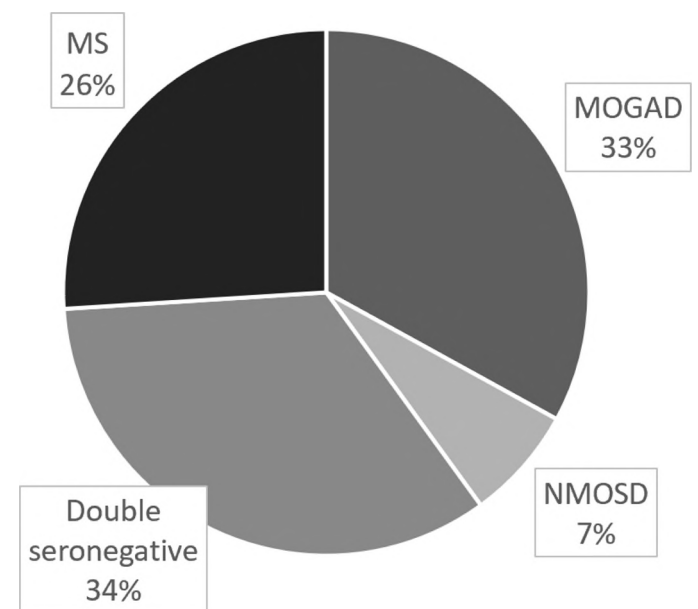MOG-IgG positive patients were the youngest group with a median

Fig. 2. Distribution of patients depending on the antibody status and diagnosis of MS and NMOSD

Table 1
Demographic and clinical status and spinal MRI features according to antibody status and diagnosis

	MOGAD (n=33)	NMOSD[1] (n=7)	Seronegative TM[2] (n=34)	MS (n=26)	P-value (corrected)[3]
Females	14/33 (42%)	6/7 (86%)	14/34 (41%)	20/26 (77%)	0.006 (ns)[5]
Age (years)[4]	7 (5-10)	12 (4-13)	9 (6-13)	15 (14-16)	<0.001 (***)[6]
Polysymptomatic	30/33 (91%)	7/7 (100%)	28/34 (82%)	16/26 (62%)	0.017 (ns)[5]
CSF cell count/μl[4]	84 (27-145)	20 (8-48)	14 (1-50)	11 (3-27)	<0.001 (***)[6]
CSF OCB	4/32 (13%)	0/7 (0%)	3/30 (10%)	23/24 (96%)	<0.001 (***)[5]
Presentation					
TM	2/33 (6%)	0/7 (0%)	6/34 (18%)	0/26 (0%)	<0.001 (***)[5]
LETM	10/33 (30%)	0/7 (0%)	25/34 (74%)	0/26 (0%)	
ADEM+TM/LETM	14/33 (42%)	0/7 (0%)	3/34 (9%)	0/26 (0%)	
MS+TM/LETM	0/33 (0%)	0/7 (0%)	0/34 (0%)	26/26 (100%)	
NMOSD+TM/LETM	7/33 (21%)	7/7 (100%)	0/34 (0%)	0/26 (0%)	
Regional					
Cervical	9/33 (27%)	1/7 (14%)	11/34 (32%)	13/26 (50%)	0.750 (ns)[5]
Thoracic	3/33 (9%)	1/7 (14%)	5/34 (15%)	2/26 (8%)	
Conus	1/33 (3%)	0/7 (0%)	1/34 (3%)	1/26 (4%)	
All of them	5/33 (15%)	0/7 (0%)	3/34 (9%)	2/26 (8%)	
Mixed	15/33 (45%)	5/7 (71%)	14/34 (41%)	8/26 (31%)	
Longitudinal lesions					
Single short	2/33 (6%)	1/7 (14%)	5/34 (15%)	13/26 (50%)	<0.001 (***)[5]
Multiple short	6/33 (18%)	0/7 (0%)	2/34 (6%)	12/26 (46%)	
LETM	18/33 (55%)	5/7 (71%)	22/34 (65%)	1/26 (4%)	
Confluent	5/33 (15%)	1/7 (14%)	3/34 (9%)	0/26 (0%)	
Mixed	2/33 (6%)	0/7 (0%)	2/34 (6%)	0/26 (0%)	
Spinal T1 lesions	3/33 (9%)	4/7 (57%)	4/34 (12%)	3/26 (12%)	0.008 (ns)[5]
Cavitation					
No lesion	30/33 (91%)	5/7 (71%)	32/34 (94%)	25/26 (96%)	0.451 (ns)[5]
In any lesion	2/33 (6%)	1/7 (14%)	1/34 (3%)	0/26 (0%)	
Hydromyelia	1/33 (3%)	1/7 (14%)	1/34 (3%)	1/26 (4%)	
Gd enhancement in selected lesions	18/30 (60%)	2/7 (29%)	8/26 (31%)	9/21 (43%)	0.130 (ns)[5]
Leptomeningeal enhancement	16/30 (53%)	0/7 (0%)	6/26 (23%)	3/21 (14%)	0.003 (*)[5]
Nerve root enhancement	4/30 (13%)	0/7 (0%)	0/26 (0%)	0/21 (0%)	0.056 (ns)[5]
Axial cord					
White matter	1/33 (3%)	0/6 (0%)	3/33 (9%)	6/25 (24%)	<0.001 (**)[5]
Grey matter	24/33 (73%)	3/6 (50%)	14/33 (42%)	2/25 (8%)	
Both	8/33 (24%)	3/6 (50%)	16/33 (48%)	17/25 (68%)	
Edema	11/33 (33%)	3/7 (43%)	6/34 (18%)	3/26 (12%)	0.110 (ns)[5]

[1] AQP4 positive and seronegative NMOSD
[2] negative MOG-IgG and AQP4-IgG
[3] p-values corrected for 16 comparisons are shown in parenthesis, ns = statistically not significant (p>0.05), * p<0.05, ** p<0.01, *** p<0.001
[4] median (interquartile range)
[5] calculated using the Chi square test
[6] calculated using the Kruskal-Wallis test. Regional = regional involvement; Axial cord = Axial cord involvement.

age of seven (interquartile range (IQR) 5-10) years at onset, followed by double seronegative children (group 3) and a median of nine (IQR 6-13) years. Children with NMOSD had a median age of 12 (IQR 4-13) years at initial presentation, while patients with MS constituted the oldest subgroup with a median age of 15 (IQR 14-16) years (p<0.001). A common symptom of patients in our cohort who were younger than two years and diagnosed with an ADS (n=5) was muscle hypotonia and weakness of the limbs (n=4). Two children also presented with cranial neuropathies. 2/5 (40%) patients were double seronegative, 2/5 (40%) were positive for MOG-IgG and 1/5 (20%) had a NMOSD.

Comparing the four groups, children with MOG-IgG had the highest average CSF cell count (84 cells/μl; range 27-145 cells/μl; p<0.001) but were only rarely positive for OCBs (4/32; 13%; p<0.001). MS patients had the lowest CSF cell count (11 cells/μl; range 3-27 cells/μl) and the highest rate of positive OCBs (23/24; 96%). Children with NMOSD had a median CSF cell count of 20 cells/μl (range 8-48 cells/μl) and no OCBs (0/7). Double seronegative patients had an average of 14 cells/μl (range 1-50 cells/μl) and were positive for OCBs only in 10% (3/30). MOG-IgG positive children mainly presented with TM/LETM as part of ADEM (14/33; 42%), with isolated LETM (10/33; 30%), or with NMOSD-MOGAD (7/33; 21%; p<0.001). Double seronegative patients often had an isolated LETM (25/34; 74%) followed by isolated TM (6/34; 18%; p<0.001).

At the beginning of our study, we excluded two children who presented with similar symptoms to patients with an ADS, such as gait ataxia, muscle weakness and incomplete paraplegia but were later diagnosed with GBS, two further patients with mental status changes and paraesthesias were diagnosed with NMDA-receptor encephalitis and neuroborreliosis respectively. All had spinal cord involvement in the MRI examination suggestive of TM but were negative for MOG-IgG and AQP4-IgG. We decided to exclude these patients because of the potential bias of dual pathology.

3.2. MR imaging of the spine in children with MOGAD, NMOSD, MS and double seronegative TM

Spinal imaging of MOG-IgG positive children was often characterised by longitudinal extensive (18/33; 55%), multiple short (6/33; 18%) or whole cord confluent lesions (5/33; 15%) and less frequently by single short lesions (2/33; 6%) compared to children with MS who often had single short (13/26; 50%) or multiple short lesions (12/26; 46%). Children with NMOSD had similar features in the spinal MRI compared to MOG-IgG positive children: 5/7 (71%) children presented with LETM. Double seronegative patients mainly presented with LETM as well (22/34; 65%), followed by single short lesions (5/34; 15%; p<0.001).

In 24/33 (73%) of children with MOGAD only the grey matter was affected. Less often white matter was affected in addition to grey matter (8/33; 24%); isolated white matter affection was only seen in one patient (1/33; 3%). In comparison, axial T2 lesions of MS patients often involved both grey and white matter (17/25; 68%) and in 6/25 (24%)

only the white matter was affected. 16/33 (48%) of double seronegative patients with TM had an involvement of both grey and white matter and in 14/33 (42%) grey matter was affected alone. Patients with NMOSD had either an involvement of only grey matter (3/6; 50%) or both grey and white matter (3/6; 50%; p<0.001).

No significant difference between the four groups concerning location of lesions, occurrence of spinal T1 lesions, cavitation, edema, or lesional contrast enhancement was found. Frequency of conus lesions in children with MOGAD, MS and double seronegative TM were similar. In children with NMOSD, no conus lesions were noted. Leptomeningeal enhancement was noted in 16/30 children with MOGAD (53%; p=0.003). In addition, 4/16 (13%; p=0.056) children with MOGAD had nerve root enhancement. In children with MS, leptomeningeal enhancement was seen in 3/21 (14%) but no nerve root enhancement. Leptomeningeal or nerve root enhancement was not detected in children with NMOSD. In children with double seronegative TM leptomeningeal enhancement was noted in 23% (6/26) and no additional nerve root enhancement was present.

3.3. MR imaging of the brain in children with MOGAD, NMOSD, MS and double seronegative TM

All patients with MS had cerebral lesions (24/24; 100%; p<0.001; Table 2), which were usually smaller than 2 cm in diameter (21/24; 88%; p<0.001) and located supratentorial (24/24; 100%; p<0.001) as well as infratentorial (15/24; 63%; p<0.001). In MOG-IgG positive patients additional brain lesions were also often noted (20/30; 67%), which were more likely supratentorial (20/30; 67%) than infratentorial

(10/30; 33%) and varying in size (8/30; 27% lesions smaller than 2 cm, 8/30; 27% lesions larger than 2 cm, 4/30; 13% lesions both smaller and larger than 2 cm). Children with NMOSD usually presented with less than 10 brain lesions (5/7; 71%), which were often smaller than 2 cm (4/7; 57%). Double seronegative patients were less likely to have brain lesions (10/33; 30%). Lesions of double seronegative children appeared either poorly demarcated (6/33; 18%) or MS-like (3/33; 9%). Lesions of children with MOGAD (17/30; 57%) and NMOSD (4/7; 57%) were mainly poorly demarcated (p<0.001). Out of the available cerebral MRIs 10/12 patients with MOG-IgG positive ADEM and 2/3 children with seronegative ADEM showed the typical brain features with large hazy, bilateral wide spread lesions.

T1 hypointense lesions were found in the majority of MS patients (21/24; 88%) but were also present albeit to a lesser extent in the other three groups: 8/30 (27%) of MOGAD, 3/7 (43%) of NMOSD and 7/33 (21%) of double seronegative patients (p<0.001).

Lesions of children with NMOSD had no Gd enhancement (0/5), whereas 50% of MS patients had contrast enhancing brain lesions (12/24; p<0.001). Lesions in the periventricular white matter (18/24; 75%; p<0.001), corpus callosum (15/24; 63%; p<0.001) and cerebellum (11/24; 46%; p<0.001) were more often found in children with MS and less likely present in the other groups. Brainstem lesions were present in 54% of children with MS (13/24) but also in 57% in children with NMOSD (4/7; p=0.001). There were no significant differences between the four groups regarding the occurrence of diffusion restriction or deep grey matter lesions. Figs. 3 and 4 show examples of the typical MRI features of each group.

Table 2
Cerebral MRI features according to antibody status and diagnosis

	MOGAD (n=30)	NMOSD[1] (n=7)	Seronegative TM[2] (n=33)	MS (n=24)	P-value (corrected)[3]
Brain lesions					
None	10/30 (33%)	2/7 (29%)	23/33 (70%)	0/24 (0%)	<0.001 (***)
1-10 lesions	11/30 (37%)	5/7 (71%)	5/33 (15%)	11/24 (46%)	
>10 lesions	9/30 (30%)	0/7 (0%)	5/33 (15%)	13/24 (54%)	
Supratentorial lesions					
None	10/30 (33%)	5/7 (71%)	24/33 (73%)	0/24 (0%)	<0.001 (***)
1-10 lesions	11/30 (37%)	2/7 (29%)	4/33 (12%)	12/24 (50%)	
>10 lesions	9/30 (30%)	0/7 (0%)	5/33 (15%)	12/24 (50%)	
Infratentorial lesions					
None	20/30 (67%)	3/7 (43%)	29/33 (88%)	9/24 (38%)	<0.001 (**)
1-10 lesions	10/30 (33%)	4/7 (57%)	4/33 (12%)	11/24 (46%)	
>10 lesions	0/30 (0%)	0/7 (0%)	0/33 (0%)	4/24 (17%)	
Brain lesions					
None	10/30 (33%)	2/7 (29%)	23/33 (70%)	0/24 (0%)	<0.001 (***)
0-2cm	8/30 (27%)	4/7 (57%)	7/33 (21%)	21/24 (88%)	
>2cm	8/30 (27%)	1/7 (14%)	3/33 (10%)	0/24 (0%)	
Both	4/30 (13%)	0/7 (0%)	0/33 (0%)	3/24 (13%)	
Brain lesions					
None	10/30 (33%)	2/7 (29%)	23/33 (70%)	0/24 (0%)	<0.001 (***)
Poorly demarcated	17/30 (57%)	4/7 (57%)	6/33 (18%)	0/24 (0%)	
Confluent	1/30 (3%)	0/7 (0%)	1/33 (3%)	0/24 (0%)	
MS-like	2/30 (7%)	1/7 (14%)	3/33 (9%)	24/24 (100%)	
Poorly&well demarc	0/30 (0%)	0/7 (0%)	0/33 (0%)	0/24 (0%)	
Diffusion restriction	0/28 (0%)	0/6 (0%)	1/32 (3%)	1/23 (4%)	0.716 (ns)
T1 hypointense	8/30 (27%)	3/7 (43%)	7/33 (21%)	21/24 (88%)	<0.001 (***)
Gd enhancement	3/28 (11%)	0/5 (0%)	2/24 (8%)	12/24 (50%)	<0.001 (**)
Periventricular WM	5/30 (17%)	1/7 (14%)	4/33 (12%)	18/24 (75%)	<0.001 (***)
Corpus callosum	2/30 (7%)	0/7 (0%)	4/33 (12%)	15/24 (63%)	<0.001 (***)
Deep grey matter					
No deep grey matter	18/30 (60%)	6/7 (86%)	30/33 (91%)	17/24 (71%)	0.172 (ns)
Thalamus	6/30 (20%)	0/7 (0%)	1/33 (3%)	3/24 (13%)	
Basal ganglia	2/30 (7%)	1/7 (14%)	2/33 (6%)	2/24 (8%)	
Both	4/30 (13%)	0/7 (0%)	0/33 (0%)	2/24 (8%)	
Brainstem lesions	9/30 (30%)	4/7 (57%)	3/33 (9%)	13/24 (54%)	0.001 (*)
Cerebellar lesions	3/30 (10%)	0/7 (0%)	3/33 (9%)	11/24 (46%)	<0.001 (**)

[1] AQP4 positive and seronegative NMOSD
[2] negative MOG-IgG and AQP4-IgG
[3] calculated using the Chi square test, p-values corrected for 13 comparisons are shown in parenthesis, ns = statistically not significant (p>0.05), * p<0.05, ** p<0.01, *** p<0.001; Poorly&well demarc = poorly and well demarcated
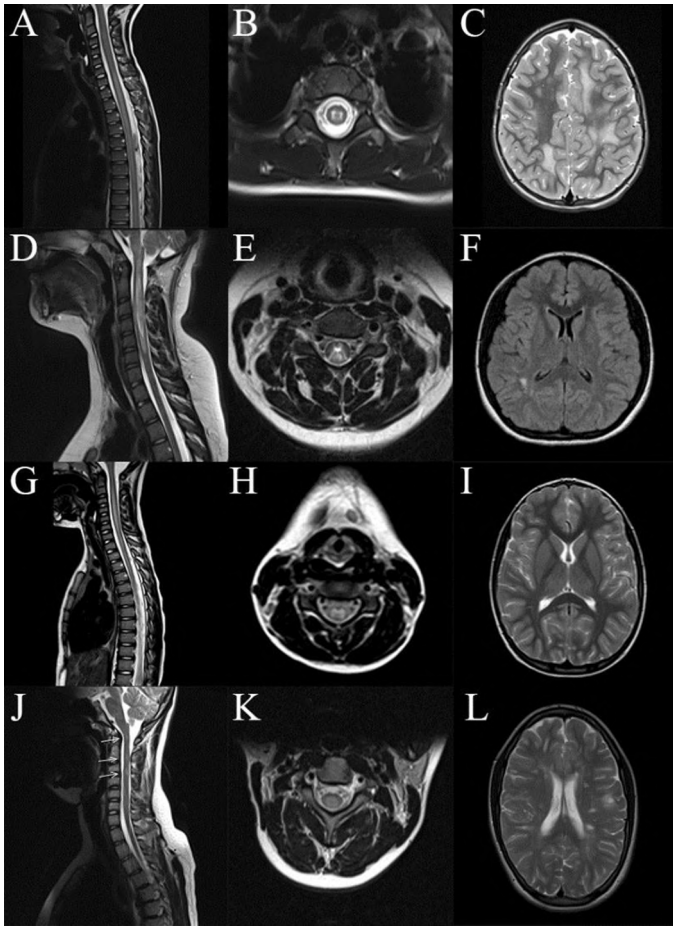
Fig. 3. Representative MR imaging features of children with MOGAD, NMOSD, double seronegative and MS patients:

Fig. 3:

(A-C): Spinal MRI of a five-year-old boy with MOG-IgG positive ADEM who presented with mental status changes and ataxia shows a LETM with a diffuse high signal intensity extending over at least eight vertebrae starting from C5 (A, sagittal T2). Axial imaging shows that the T2 changes are primarily restricted to the grey matter (H-sign, B). Brain MRI reveals the typical lesion features of ADEM: large, diffuse and hazy lesions of variable size of the white matter (C, axial T2).

(D-E): Spinal MRI of a 12-year-old girl with AQP4-IgG positive NMOSD and episodes with optic neuritis (ON) and LETM shows a long, confluent lesion stretching from the medullo-cervical junction of the spinal cord to C6 (D, sagittal T2). The lesion is accentuated around the central canal with varying signal intensities from low to high hyperintensity in T2. Corresponding axial imaging of the lesion reveals a primarily central involvement of the grey matter of the spinal cord also referred to as H-sign (E, axial T2). Axial brain imaging of a 13-year-old girl presenting with bilateral weakness of the legs and bladder dysfunction and diagnosed with AQP4-IgG positive NMOSD shows only one unspecific lesion (F, axial T2).

(G-I): Spinal MRI of a five-year-old boy with a double seronegative transverse myelitis shows a LETM (G, sagittal T2). Axial T2 image shows a hyperintense lesion affecting the grey matter but also extending bilaterally into the dorsal white matter (H). The cranial MRI – as in most other double seronegative TM – was normal (I, axial T2).

(J-L): Spinal cord imaging of a 14-year-old boy with an episode of ON who was subsequently diagnosed with MS shows three T2 hyperintense lesions (J, sagittal T2). The axial image demonstrates involvement of the entire central region of the spinal cord not only limited to the grey matter but also affecting the dorsolateral white matter (K, axial T2). Brain MRI reveals multiple hyperintense periventricular lesions (L, axial T2).

4. Discussion

From the initial cohort of children referred to our Centre with a presumed ADS, nearly 10% of children had radiological and clinical evidence of TM either alone or as part of another subtype of ADS. To better understand the distinct clinical and radiological differences, we assigned our patients with TM to four different disease subtypes including MOGAD, NMOSD, MS and double seronegative TM for further analysis. Using this approach, we could show that serum IgG antibodies against MOG were present in 1/3 of children with TM. We further found that children with MOGAD-associated TM were younger, more often had negative OCBs and a high CSF cell count, whereas children with MS were older, nearly always positive for OCBs and had a low CSF cell count. Widespread spinal involvement of children with MOG-IgG mainly occurred as part of an episode with ADEM or solely as LETM. In the NMOSD group, most children had brain lesions as well. Also, children with TM and MS always had additional cerebral lesions which were significantly less often present in double seronegative children with TM – a distinct feature of this subgroup of patients.

We further show that patients with antibodies to MOG have differing features compared to children with MS in regards to extension and axial location of spinal lesions. As shown also in previous studies, in MOG-IgG antibody positive patients mainly the grey matter is affected – usually referred to as H-sign in axial sequences – in addition to the involvement of at least three adjacent vertebral segments, whereas patients with MS usually had single or multiple short lesions and an involvement of both grey and white matter (Dubey et al., 2019, Fadda et al., 2021, Tantsis et al., 2019). Double seronegative children presented foremost with LETM with grey and white matter involvement, therefore an H-sign was less likely noted. In contrast to other studies, however, no significant differences between the four groups regarding lesion location in sagittal plane (i.e. cervical, thoracal or conus involvement) were noted (Dubey et al., 2019, Tantsis et al., 2019). Interestingly, in our cohort conus lesions were not restricted to MOGAD, thought to be a hallmark of MOGAD in contrast to AQP4-IgG positive or MS patients (Dubey et al., 2019, Fadda et al., 2021). Studies in adult patients also found an involvement of three adjacent vertebral segments in MOG-/AQP4-IgG positive patients (Dubey et al., 2019, Jarius et al., 2016, Sato et al., 2014) or double seronegative patients (Sato et al., 2014), as well as single or multiple short lesions in patients with MS (Dubey et al., 2019). Regional involvement of the spine in MOG-IgG positive adult patients varies with some studies showing particularly lumbar and conus lesions (Sato et al., 2014, Mariano et al., 2021) and some studies showing mostly cervical and thoracic lesions (Jarius et al., 2016, Ciron et al., 2020). Considering the large number in our cohort, conus lesions were not found to be a distinct feature of children with MOG-IgG. Further multi-center studies are needed to verify if the presence of conus lesions may be a helpful indicator to distinguish between different disease entities.

In a very recently published study by Fadda et al, the authors also reported that leptomeningeal enhancement of the spine was highly predictive for children with MOGAD (Fadda et al., 2021). We also detected leptomeningeal enhancement predominantly in the vicinity of the spinal lesion in a substantial number of MOG-IgG positive children which was far less often present in the other subgroups and confirm that leptomeningeal enhancement may be a special feature for the group of MOGAD. Nerve root enhancement detectable in a small group of MOGAD children was not seen in children with MS, NMOSD or double seronegative TM. Interestingly, in children with MOG-IgG antibodies and nerve root enhancement no clinical signs of a polyradiculopathy were present.

Finally, several notable differences in the lesion pattern of the brain, which may be helpful in regards to diagnosis, treatment decision and prognosis when evaluating a child with TM in the context of the first event were noted. MOG-IgG positive patients had lesions which were poorly demarcated and larger in size, whereas lesions of MS patients
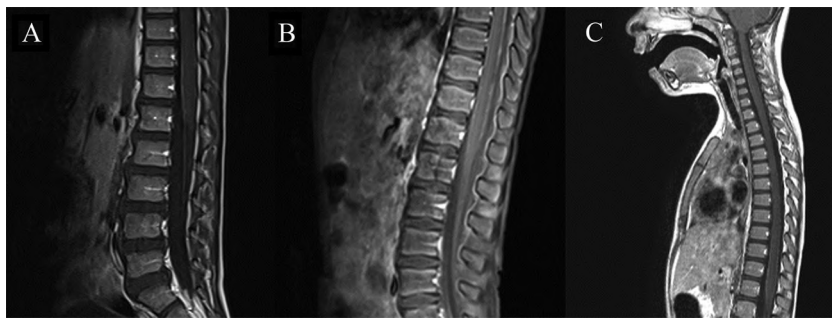
Fig. 4. Representative MR images from children with MOG-IgG and leptomeningeal and nerve root enhancement:
Fig. 4:
(A-C): MRI of the spine of a five-year-old boy with MOG-IgG positive ADEM and a LETM as detailed above (Fig.3 A-C) also revealed leptomeningeal and nerve root enhancement (A, sagittal T1 with contrast medium).
MR imaging of an eight-year-old boy with LETM shows pronounced leptomeningeal enhancement without nerve root involvement (B, sagittal T1 with contrast medium).
Three-year-old boy with MOG-IgG positive LETM with leptomeningeal enhancement at the level of the lesion (cervical) and in the region of the conus medullaris without nerve root involvement (C, sagittal T1 with contrast medium).

appeared well-demarcated, smaller in size and located in areas such as the corpus callosum (Baumann et al., 2018, Jurynczyk et al., 2017). Gd enhancement was nearly exclusively found in brain lesions of children with MS (Tantsis et al., 2019). Cerebellar lesions and T1 hypointense lesion were more frequent in children with MS, infrequent in MOGAD and double seronegative TM and absent in NMOSD. T1 hypointense lesions were a prominent feature in the majority of children with MS.

Several limitations of this study need to be addressed: We performed a retrospective study involving multiple centers. Therefore, a standardised MRI acquisition protocol could not be applied and a referral bias not revealing the true incidence of clinical entities or MRI patterns cannot be excluded as patients were sent from different institutions. Secondly, in particular for the assessment of spinal lesions, not in all patients axial imaging and STIR sequences were available and thirdly, MRI studies were performed on scanners with different field strengths, leading to a different quality of images and results. A further limitation is the small sample size of children with NMOSD. In addition, we focused on the radiological features at the initial presentation but did not include clinical follow-up data or MRI studies in order to assess the subsequent course of the different disease entities. A follow-up study is ongoing to address open questions including clinical outcome and spinal changes such as atrophy after an initial attack overtime.

5. Conclusion

Involvement of the spinal cord in children with ADS is common and revealed important radiological differences between MOGAD, NMOSD, MS and double seronegative patients. Distinct imaging features in children with MOGAD includes LETM, the H-sign, leptomeningeal enhancement and often large, hazy and bilateral cerebral lesion. Children with MS had single or multiple short spinal lesions with involvement of both grey and white matter in addition to cerebellar, corpus callosum, periventricular white matter and T1 hypointense lesions. Double seronegative children were less likely to have brain lesions at all. Knowledge of these radiological features may help in the initial diagnostic process and therapeutic decisions as long as antibody results are pending. Long-term studies are warranted looking at the radiological sequelae and evolution overtime in particular of children affected with MOGAD.

Credit author statement

Ines El Naggar: Investigation, Writing – Original Draft, Visualization **Robert Cleaveland**: Investigation, Visualization **Eva-Maria Wendel**: Resources, Data Curation **Annikki Bertolini**: Writing – Original Draft **Kathrin Schanda**: Investigation **Michael Karenfort**: Resources **Charlotte Thiels**: Resources **Adela Della Marina**: Resources **Mareike Schimmel**: Resources **Steffen Leiz**: Resources **Christian Lechner**: Resources **Matthias Baumann**: Resources **Markus Reindl**: Formal analysis **Andreas Wegener-Panzer** Investigation **Kevin Rostásy**: Conceptualization, Methodology, Supervision, Project administration, Writing – Review Editing **BIOMARKER Study Group**: Resources

Search term

(1) transverse myelitis, (2) MOG antibodies, (3) children, (4) autoimmune, (5) MS

Declaration of Competing Interest

References

Proposed diagnostic criteria and nosology of acute transverse myelitis. Neurology 59 (4), 2002, 499–505. https://doi.org/10.1212/wnl.59.4.499.

Wolf, VL, Lupo, PJ, Lotze, TE., 2012. Pediatric Acute Transverse Myelitis Overview and Differential Diagnosis. J. Child Neurol. 27 (11), 1426–1436. https://doi.org/10.1177/0883073812452916.

Barakat, N, Gorman, MP, Benson, L, Becerra, L, Borsook, D., 2015. Pain and spinal cord imaging measures in children with demyelinating disease. NeuroImage. Clinical 9, 338–347. https://doi.org/10.1016/j.nicl.2015.08.019.

Absoud, M, Greenberg, BM, Lim, M, Lotze, T, Thomas, T, Deiva, K., 2016. Pediatric transverse myelitis. Neurology 87 (9 Suppl 2), S46–S52. https://doi.org/10.1212/WNL.0000000000002820.

Hennes, E-M, Baumann, M, Schanda, K, et al., 2017. Prognostic relevance of MOG antibodies in children with an acquired demyelinating syndrome. Neurology 89 (9), 900–908. https://doi.org/10.1212/WNL.0000000000004312.

Hacohen, Y, Absoud, M, Deiva, K, et al., 2015. Myelin oligodendrocyte glycoprotein antibodies are associated with a non-MS course in children. Neurology(R) neuroimmunology & neuroinflammation 2 (2), e81. https://doi.org/10.1212/NXI.0000000000000081.

Spadaro, M, Gerdes, LA, Krumbholz, M, et al., 2016. Autoantibodies to MOG in a distinct subgroup of adult multiple sclerosis. Neurology(R) neuroimmunology & neuroinflammation 3 (5), e257. https://doi.org/10.1212/NXI.0000000000000257.

Baumann, M, Grams, A, Djurdjevic, T, et al., 2018. MRI of the first event in pediatric acquired demyelinating syndromes with antibodies to myelin oligodendrocyte glycoprotein. J. Neurol. 265 (4), 845–855. https://doi.org/10.1007/s00415-018-8781-3.

Dubey, D, Pittock, SJ, Krecke, KN, et al., 2019. Clinical, Radiologic, and Prognostic Features of Myelitis Associated With Myelin Oligodendrocyte Glycoprotein

Autoantibody. JAMA Neurol. 76 (3), 301–309. https://doi.org/10.1001/jamaneurol.2018.4053.

Hacohen, Y, Mankad, K, Chong, WK, et al., 2017. Diagnostic algorithm for relapsing acquired demyelinating syndromes in children. Neurology 89 (3), 269–278. https://doi.org/10.1212/WNL.0000000000004117.

Fadda, G, Alves, CA, O`Mahony, J, et al., 2021. Comparison of Spinal Cord Magnetic Resonance Imaging Features Among Children With Acquired Demyelinating Syndromes. JAMA network open 4 (10), e2128871. https://doi.org/10.1001/jamanetworkopen.2021.28871.

Lechner, C, Baumann, M, Hennes, E-M, et al., 2016. Antibodies to MOG and AQP4 in children with neuromyelitis optica and limited forms of the disease. J. Neurol. Neurosurg. Psychiatry 87 (8), 897–905. https://doi.org/10.1136/jnnp-2015-311743.

Mader, S, Gredler, V, Schanda, K, et al., 2011. Complement activating antibodies to myelin oligodendrocyte glycoprotein in neuromyelitis optica and related disorders. Journal of neuroinflammation 8, 184. https://doi.org/10.1186/1742-2094-8-184.

Wingerchuk, DM, Banwell, B, Bennett, JL, et al., 2015. International consensus diagnostic criteria for neuromyelitis optica spectrum disorders. Neurology 85 (2), 177–189. https://doi.org/10.1212/WNL.0000000000001729.

Thompson, AJ, Banwell, BL, Barkhof, F, et al., 2018. Diagnosis of multiple sclerosis: 2017 revisions of the McDonald criteria. The Lancet Neurology 17 (2), 162–173. https://doi.org/10.1016/S1474-4422(17)30470-2.

Tantsis, EM, Prelog, K, Alper, G, et al., 2019. Magnetic resonance imaging in enterovirus-71, myelin oligodendrocyte glycoprotein antibody, aquaporin-4 antibody, and multiple sclerosis-associated myelitis in children. Dev. Med. Child Neurol. 61 (9), 1108–1116. https://doi.org/10.1111/dmcn.14114.

Jarius, S, Ruprecht, K, Kleiter, I, et al., 2016. MOG-IgG in NMO and related disorders: a multicenter study of 50 patients. Part 2: Epidemiology, clinical presentation, radiological and laboratory features, treatment responses, and long-term outcome. Journal of neuroinflammation 13 (1), 280. https://doi.org/10.1186/s12974-016-0718-0.

Sato, DK, Callegaro, D, Lana-Peixoto, MA, et al., 2014. Distinction between MOG antibody-positive and AQP4 antibody-positive NMO spectrum disorders. Neurology 82 (6), 474–481. https://doi.org/10.1212/WNL.0000000000000101.

Mariano, R, Messina, S, Roca-Fernandez, A, Leite, MI, Kong, Y, Palace, JA., 2021. Quantitative spinal cord MRI in MOG-antibody disease, neuromyelitis optica and multiple sclerosis. Brain a journal of neurology 144 (1), 198–212. https://doi.org/10.1093/brain/awaa347.

Ciron, J, Cobo-Calvo, A, Audoin, B, et al., 2020. Frequency and characteristics of short versus longitudinally extensive myelitis in adults with MOG antibodies: A retrospective multicentric study. Mult. Scler. 26 (8), 936–944. https://doi.org/10.1177/1352458519849511.

Jurynczyk, M, Geraldes, R, Probert, F, et al., 2017. Distinct brain imaging characteristics of autoantibody-mediated CNS conditions and multiple sclerosis. Brain a journal of neurology 140 (3), 617–627. https://doi.org/10.1093/brain/aww350.